Singularly perturbed initial-boundary value problems with a pulse in the initial condition

José Luis Gracia and Eugene O'Riordan

Abstract A singularly perturbed parabolic equation of reaction-diffusion type is examined. Initially the solution approximates a concentrated source, which causes an interior layer to form within the solution for all future times. Combining a classical finite difference operator with a layer-adapted mesh, parameter-uniform convergence is established. Numerical results are presented to illustrate the theoretical error bounds.

1 Introduction

In [4], a singularly perturbed parabolic problem, of convection diffusion type,

$$-\varepsilon u_{xx} + a u_x + b u + c u_t = f, \quad \varepsilon, a(x,t), b(x,t), c(x,t) > 0,$$

with a layer (having a Gaussian profile) present in the initial condition $u(x,0) = \phi(x;\varepsilon)$, was examined. The initial layer induced an interior layer in the solution of the parabolic problem. To establish that the numerical method (constructed in [4]) was parameter-uniform [2], the scale of the interior layer was set to be of order $O(\varepsilon)$; in other words, the scale of the initial layer corresponded to the scale of any boundary layer present in the solution. In this paper, we examine the possibility of an initial layer of a different scale being transported through time. To simplify the matter, we consider a parabolic problem with no convection present. In order to retain parameter-uniform convergence, it is established below that the layer width in

José Luis Gracia
Department of Applied Mathematics, University of Zaragoza, Spain e-mail: jlgracia@unizar.es.
The research of this author was partly supported by the Institute of Mathematics and Applications (IUMA), the project MTM2016-75139-R and the Diputación General de Aragón.

Eugene O'Riordan
School of Mathematical Sciences, Dublin City University, Ireland e-mail: eugene.oriordan@dcu.ie

the initial condition can have a scale wider than the scale induced by the differential equation. However, if the scale of the initial layer is significantly thinner than the scale of any boundary layer then the rate of convergence is adversely effected by the presence of such an excessively thin layer in the initial condition, when a uniform mesh in time is utilized in the numerical method. Numerical results for a numerical method utilizing a particular piecewise-uniform mesh in both space and time suggest a potential improvement in the convergence rate in the case of a very thin pulse. In this paper C denotes a generic constant that is independent of the parameter ε and the mesh parameters N and M. For any function z, we set $\|z\|_{\bar{G}} := \max_{(x,t)\in\bar{G}} |z(x,t)|$.

2 Reaction-diffusion problem

Consider the following singularly perturbed parabolic problem of reaction-diffusion type : Find u such that

$$Lu := (-\varepsilon u_{xx} + bu + cu_t)(x,t) = f(x,t),\ (x,t) \in \Omega := (-1,1)\times(0,T], \quad \text{(1a)}$$

$$u(x,0) = g_1(x) + g_2(x)e^{-\theta\frac{x^2}{\varepsilon}}, -1 \le x \le 1, \quad \theta > 0; \quad \text{(1b)}$$

$$u(-1,t) = \phi_L(t),\ u(1,t) = \phi_R(t),\ 0 < t \le T, \quad b(x,t) \ge 0,\ c(x,t) > 0; \quad \text{(1c)}$$

$$g_2^{(i)}(-1) = g_2^{(i)}(1) = 0, \qquad i = 0,1,2; \quad \text{(1d)}$$

where $b(x,t), c(x,t), f(x,t), g_1(x), g_2(x)$ are sufficiently smooth functions. In this problem, in contrast to the case of a convection-diffusion problem [4], there are no immediate restrictions on the final time T, as the interior layer will not interact with the boundaries of the domain. However, the bounds in the final error estimate given in Theorem 2 do depend on $e^{\theta T}$ and hence, for $\theta > 1$, these bounds become large as T increases.

To highlight the interplay between the width of the pulse and the scale of the layers emanating from the presence of the singular perturbation parameter in the differential equation, we consider the following simple problem

$$-\varepsilon u_{xx} + u_t = 0, \quad (x,t) \in Q := (-1,1)\times(0,0.5], \quad \text{(2a)}$$

$$u(x,0) = (1-x^2)^2 e^{-\frac{\theta x^2}{\varepsilon}},\ -1 \le x \le 1; \quad u(0,t) = u(1,t) = 0,\ 0 < t \le 0.5. \quad \text{(2b)}$$

A closed form representation of the solution of this problem is

$$u(x,t) = \frac{1}{2\sqrt{\varepsilon\pi t}} e^{-\frac{\theta x^2}{\varepsilon(1+4\theta t)}} \int_{s=-1}^{1} (1-s^2)^2 e^{-\frac{(1+4\theta t)}{4\varepsilon t}\left(\frac{x}{1+4\theta t} - s\right)^2}\, ds.$$

As $\frac{\varepsilon}{\theta} \to 0^+$, we note that the solution behaves like

$$u(x,t) \to \frac{1}{\sqrt{1+4\theta t}} e^{-\frac{\theta x^2}{\varepsilon(1+4\theta t)}} \left(1 - \frac{x^2}{(1+4\theta t)^2}\right)^2.$$

Observe that the layer width initially is visible in the bound

$$e^{-\frac{\theta x^2}{\varepsilon}} \leq e^{-\frac{\theta x^2}{\varepsilon(1+4\theta t)}} \leq e^{-\frac{\theta x^2}{2\varepsilon}}, \qquad 0 < t \leq \frac{1}{4\theta};$$

and the range of applicability for this inequality increases as the value of θ decreases. For any $\theta \geq 1$ we also have, for intermediate values of time, that

$$e^{-\frac{x^2}{\varepsilon}} \leq e^{-\frac{\theta x^2}{\varepsilon(1+4\theta t)}} \leq e^{-\frac{x^2}{2\varepsilon}}, \qquad \frac{1}{4} - \frac{1}{4\theta} \leq t \leq \frac{1}{2} - \frac{1}{4\theta}, \qquad \theta \geq 1.$$

The layer width associated with the function $e^{-\frac{\theta x^2}{\varepsilon(1+4\theta t)}}$ evolves from an initial width of $\mathscr{O}(\sqrt{\varepsilon/\theta})$ to a width of $\mathscr{O}(\sqrt{\varepsilon})$ as time increases, in the case where $\theta \geq 1$. In the case where $\theta < 1$, we simply have

$$e^{-\frac{x^2}{5t\varepsilon}} \leq e^{-\frac{\theta x^2}{\varepsilon(1+4\theta t)}} \leq e^{-\frac{x^2}{6t\varepsilon}}, \qquad \frac{1}{2\theta} \leq t \leq \frac{1}{\theta}.$$

Over a finite time range $4T\theta \leq 1$, there will be no significant change in the layer width for $\theta < 1$. In both cases $\theta < 1, \theta \geq 1$, note that the amplitude of the pulse at $x = 0$ decreases with time and with respect to θ. This effect is illustrated in the two figures displayed in Figure 1. Finally, note that $u_t(0,0) < 0$, but $u_t(x,0) > 0,\ x \in$

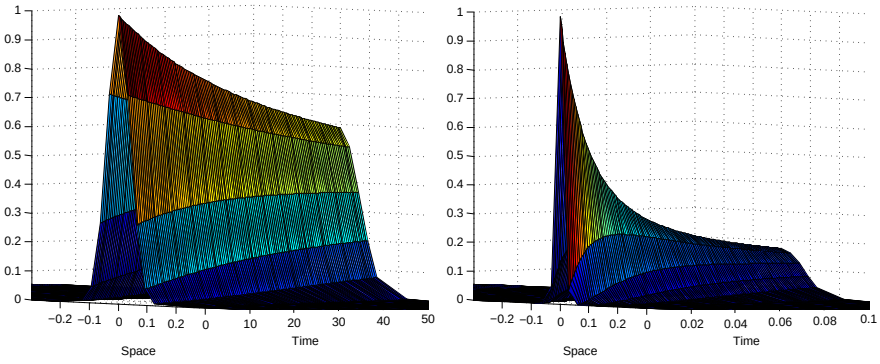

Fig. 1 Problem (2): Zoom into the interior layer region of the computed solution $U^{N,M}$ generated by the numerical scheme (5) for $N = 32, M = 128$. In the left figure, $\theta = 0.01, T = 50$ and $\varepsilon = 2^{-15}$ and in the right figure $\theta = 100, T = 0.1$ and $\varepsilon = 2^{-5}$.

$(-1,1) \setminus (-C\sqrt{\varepsilon/\theta}, C\sqrt{\varepsilon/\theta})$. Hence, the initial time derivative has different signs within and outside the layer region.

In our subsequent numerical analysis, we shall see that a piecewise-uniform Shishkin mesh, with a transition point related to the width of the pulse, coupled with a uniform mesh in time, suffices to obtain parameter-uniform convergence only in the case where $\theta \leq 1$.

3 Bounds on the derivatives of the continuous solution

The general solution of (1) can be decomposed into the sum $u = v + w_L + w_R + z$, where $v, w_L, w_R, z \in \mathscr{C}^{4+\gamma}(\bar{\Omega})$ and

$$\begin{aligned} Lv &= f, \;\; v(x,0) = g_1(x), \quad v(-1,t), v(1,t) \quad \text{suitably chosen;} \\ Lw_L &= 0, \;\; w_L(-1,t) = (u-v)(-1,t), \quad w_L(1,t) = 0, \; w_L(x,0) = 0; \\ Lw_R &= 0, \;\; w_R(1,t) = (u-v)(1,t), \quad w_R(-1,t) = 0, \; w_R(x,0) = 0; \\ Lz &= 0, \;\; z(x,0) = g_2(x)e^{-\theta\frac{x^2}{\varepsilon}}, \quad z(-1,t) = z(1,t) = 0. \end{aligned}$$

For the regular and boundary layer components the following bounds can be established, as in [6]: For $0 \le j + 2m =: n \le 4$,

$$\left\| \frac{\partial^{j+m} v}{\partial x^j \partial t^m} \right\|_{\Omega} \le C\left(1 + \varepsilon^{1-j/2}\right), \tag{3a}$$

$$\left| \frac{\partial^{j+m} w_L}{\partial x^j \partial t^m}(x,t) \right| \le C\varepsilon^{-j/2} e^{-\frac{(1+x)}{\sqrt{\varepsilon}}}, \qquad \left| \frac{\partial^{j+m} w_R}{\partial x^j \partial t^m}(x,t) \right| \le C\varepsilon^{-j/2} e^{-\frac{(1-x)}{\sqrt{\varepsilon}}}. \tag{3b}$$

In passing we note that the interior layer component z is smoother than in the case of the convection-diffusion problem [4] as $[z](0,t) = [z_x](0,t) = 0$.

Theorem 1. *Assume that $\theta T \le C$ and $\theta \ge C\varepsilon$. For $0 \le j + 2m =: n \le 4$,*

$$|z(x,t)| \le Ce^{\theta t/c_0} e^{-\frac{\sqrt{\theta}|x|}{\sqrt{\varepsilon}}}, \tag{4a}$$

$$\left\| \frac{\partial^{j+m} z}{\partial x^j \partial t^m} \right\|_{\Omega} \le Ce^{\theta T/c_0}(1 + \theta^{n/2})\varepsilon^{-j/2}, \tag{4b}$$

where $c_0 := \min c(x,t)$. In addition, if $C\varepsilon \le \theta \le 1$, then

$$\left\| \frac{\partial^{j+m} z}{\partial x^j \partial t^m} \right\|_{\Omega} \le C\varepsilon^{-j/2}\theta^{j/2}. \tag{4c}$$

Proof. From the maximum principle, $|z(x,t)| \le Ce^{\frac{t}{c_0}}$, $\forall (x,t) \in \Omega$. Note that for all s and any $\kappa > 0$

$$e^{-\kappa s^2} \le e^{\frac{1}{4}} e^{-\sqrt{\kappa}|s|}.$$

Then using the obvious barrier functions, we establish the bounds (4a) on z separately on $\Omega^- = [-1,0] \times [0,T]$ and $\Omega^+ = [0,1] \times [0,T]$, while noting that $|z(0,t)| \le Ce^{\frac{t}{c_0}}$ has been already established. In order to obtain parameter-explicit bounds on the derivatives of z in the entire region Ω, and to deal with the cases of $c\varepsilon \le \theta < 1$ and $\theta \ge 1$ together, we introduce the stretched variables

$$\eta := \frac{\sqrt{\theta_*}x}{\sqrt{\varepsilon}}, \quad \tau = \theta_* t \;\text{ with }\; \theta_* := \max\{1, \theta\} \;\text{ and }\; \check{u}(\eta,\tau) := \hat{u}(s,t).$$

Hence the differential equation can be written in the form

$$-\check{z}_{\eta\eta}+\frac{\check{b}}{\theta_*}\check{z}+\check{c}\check{z}_{\tau}=0,\quad (\eta,\tau)\in\left(-\sqrt{\theta_*}/\sqrt{\varepsilon},\sqrt{\theta_*}/\sqrt{\varepsilon}\right)\times(0,\theta_* T],$$

with zero boundary conditions and an initial condition of the form

$$\check{z}(\eta,0)=g_2\left(\sqrt{\varepsilon}\eta/\sqrt{\theta}\right)e^{-\eta^2}\ \text{ if }\ \theta_*=\theta,\ \text{ and }\ \check{z}(\eta,0)=g_2(\sqrt{\varepsilon}\eta)e^{-\theta\eta^2}\ \text{ if }\ \theta_*=1.$$

To obtain bounds on the derivatives of the interior layer, we now use the interior estimates from [5, p. 352], to deduce that

$$\left|\frac{\partial^{j+m}\check{z}}{\partial\eta^j\partial\tau^m}(\eta,\tau)\right|\le Ce^{\theta T/c_0}+C\left|\frac{\partial^j\check{z}}{\partial\eta^j}(\eta,0)\right|.$$

Returning to the original variables, we get

$$\left\|\frac{\partial^{j+m}z}{\partial x^j\partial t^m}\right\|_{\Omega}\le Ce^{\theta T/c_0}\theta^m\left(\frac{\theta}{\varepsilon}\right)^{j/2}\left(1+\sqrt{\frac{\varepsilon}{\theta}}\right)^j\le Ce^{\theta T/c_0}\theta^{(j+2m)/2}\varepsilon^{-j/2},\quad \text{if } \theta_*=\theta,$$

$$\left\|\frac{\partial^{j+m}z}{\partial x^j\partial t^m}\right\|_{\Omega}\le Ce^{\theta T/c_0}\varepsilon^{-j/2}\left(\sqrt{\varepsilon}+\sqrt{\theta}\right)^j\le Ce^{\theta T/c_0}\varepsilon^{-j/2}\theta^{j/2},\quad \text{if } \theta_*=1.$$

In the last inequality we have used the fact that $C\varepsilon\le\theta$.

Remark 1. Note that in the case where $\theta\le C\varepsilon$, then in the above proof, we can replace θ_* by θ and consequently deduce that all the partial derivatives of z are uniformly bounded. Thus, when $\theta\le C\varepsilon$, there is no interior layer present.

4 Numerical method and error analysis

We employ a classical fully implicit finite difference operator on a piecewise - uniform Shishkin mesh [2]. The finite difference scheme is given by

$$L^{N,M}U:=-\varepsilon\delta_x^2U+bU+cD_t^-U=f(x_i,t_j),\quad (x_i,t_j)\in\Omega^{N,M},\tag{5a}$$

$$U(x_i,0)=u(x_i,0),\quad U(-1,t_j)=u(-1,t_j),\ U(1,t_j)=u(1,t_j).\tag{5b}$$

Note that nothing special is required at the mesh points $(0,t_j)$, where the interior layer is located. Based on the above bounds on the layer components of the solution, we split the space domain $[-1,1]$ into the five subintervals

$$[-1,-1+\sigma_R]\cup[-1+\sigma_R,-\tau]\cup[-\tau,\tau]\cup[\tau,1-\sigma_R]\cup[1-\sigma_R,1],\tag{5c}$$

$$\tau:=\min\left\{\frac{1}{8},2\frac{\sqrt{\varepsilon}}{\sqrt{\theta}}\ln N\right\},\ \sigma_R:=\min\left\{\frac{1}{8},2\sqrt{\varepsilon}\ln N\right\},\tag{5d}$$

where N is the spatial discretisation parameter. The grid points, in space, are uniformly distributed within each subinterval such that

$$-x_0 = x_N = 1,\ -x_{N/8} = x_{7N/8} = 1-\sigma_R,\ -x_{3N/8} = x_{5N/8} = \tau,\ x_{N/2} = 0.$$

We use M mesh elements uniformly distributed in time and the mesh $\bar{\Omega}^{N,M}$ is the tensor product of the spatial and time meshes.

The discrete counterparts of the components v, w_L, w_R and z are denoted by V, W_L, W_R and Z, which are defined in a standard way. Bounds on the errors in the discrete regular component (V), boundary layers components (W_L and W_R) follow from a standard truncation argument and suitable barrier functions [1, 6]. Thus, we have that

$$\|V-v\|_{\bar{\Omega}^{N,M}} \le C(N^{-1}\ln N)^2 + CM^{-1}, \quad \|W_L - w_L\|_{\bar{\Omega}^{N,M}} \le CN^{-2} + CM^{-1}, \quad (6)$$

and the boundary layer component W_R satisfies similar error estimates as W_L. For $M \ge \mathcal{O}(\ln(N))$, the discrete interior layer function satisfies the bounds

$$(a) \qquad |Z(x_i,t_j)| \le Ce^{\theta T/c_0} \prod_{k=i}^{N/2} \left(1 + \frac{\sqrt{\theta}h_k}{2\sqrt{\varepsilon}}\right), \quad x_i \le 0,$$

$$(b) \qquad |Z(x_i,t_j)| \le Ce^{\theta T/c_0} \prod_{k=N/2}^{i} \left(1 + \frac{\sqrt{\theta}h_k}{2\sqrt{\varepsilon}}\right)^{-1}, \quad x_i \ge 0,$$

where $h_k := x_k - x_{k-1}$, for $k = 1,2,\ldots,N$. From these bounds we establish that when $8\tau < 1$

$$|Z(x_i,t_j)| \le Ce^{\theta T/c_0} N^{-2}, \quad x_i \in (-1,1)\setminus(-\tau,\tau).$$

In addition, for $x_i \in (-\tau,\tau)$

$$|L^{N,M}(Z-z)(x_i,t_j)| \le \begin{cases} Ce^{\theta T/c_0}\left(\theta(N^{-1}\ln N)^2 + \theta^2 M^{-1}\right), & \text{if } 1 \le \theta, \\ Ce^{\theta T/c_0}\left(\theta(N^{-1}\ln N)^2 + M^{-1}\right), & \text{if } \theta < 1. \end{cases}$$

Using a suitable barrier function we deduce that

$$\|Z-z\|_{(-\tau,\tau)} \le \begin{cases} Ce^{\theta T/c_0}\left(\theta(N^{-1}\ln N)^2 + \theta^2 M^{-1}\right), & \text{if } 1 \le \theta, \\ Ce^{\theta T/c_0}\left(\theta(N^{-1}\ln N)^2 + M^{-1}\right), & \text{if } \theta < 1. \end{cases} \quad (7)$$

From the error bounds (6) and (7), the following nodal error bound follows by the triangular inequality.

Theorem 2. *Assume $M \ge \mathcal{O}(\ln(N))$. Let be U the solution of the discrete problem* (5) *and u the solution of the continuous problem* (1)*. Then,*

$$\|U-u\|_{\bar{\Omega}^{N,M}} \le \begin{cases} Ce^{\theta T/c_0}\left(\theta(N^{-1}\ln N)^2 + \theta^2 M^{-1}\right), & \textit{if } 1 \le \theta, \\ Ce^{\theta T/c_0}\left((N^{-1}\ln N)^2 + M^{-1}\right), & \textit{if } \theta < 1. \end{cases}$$

5 Numerical experiments

Consider the following test problem

$$-\varepsilon u_{xx} + u + u_t = (1-x^2)t, \quad (x,t) \in Q := (-1,1) \times (0,1], \tag{8}$$
$$u(x,0) = (1-x^2)^2(1+x)^2 e^{-\frac{\theta x^2}{\varepsilon}}, \ -1 \le x \le 1, \ u(0,t) = u(1,t) = 0, \ 0 < t \le 1,$$

where we shall consider some sample values for the parameter θ. In Figures 2 and 3 we display the computed solutions generated by the numerical scheme (5) with $\varepsilon = 2^{-5}, 2^{-10}$ and $N = M = 32$. The values of the parameter θ in the initial condition are $\theta = 1, 100$ and we observe again the influence of this parameter in the profile of the solution. Note that the time derivative $|u_t(0,0)|$ increases with θ.

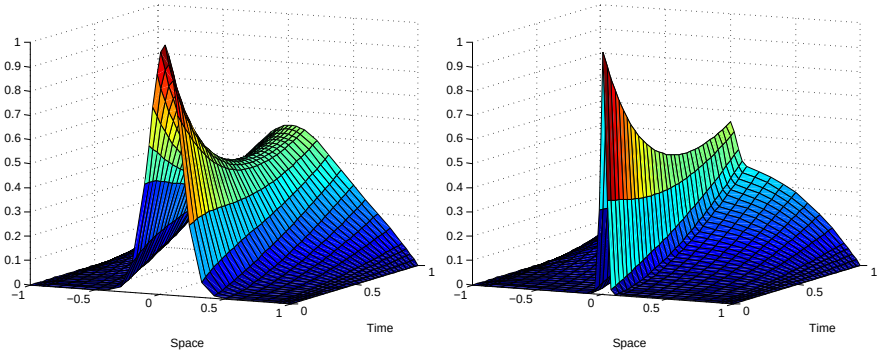

Fig. 2 Test problem (8): Computed solution $U^{N,M}$ generated by the numerical scheme (5) for $N = M = 32$, $\theta = 1$ and $\varepsilon = 2^{-5}$ (left figure) and $\varepsilon = 2^{-10}$ (right figure)

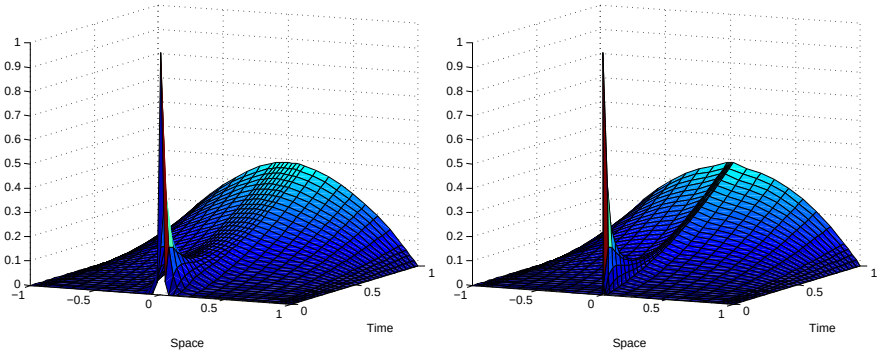

Fig. 3 Test problem (8): Computed solution $U^{N,M}$ generated by the numerical scheme (5) for $N = M = 32$, $\theta = 100$ and $\varepsilon = 2^{-5}$ (left figure) and $\varepsilon = 2^{-10}$ (right figure)

The exact solution of this problem is unknown and we use the two-mesh principle [2] to estimate the orders of convergence by first computing the two-mesh differences

$$F_\varepsilon^{N,M} := \max\left\{\|U^{N,M} - \bar{U}^{2N,2M}\|_{\bar{\Omega}^{N,M}}, \|\bar{U}^{N,M} - U^{2N,2M}\|_{\bar{\Omega}^{2N,2M}}\right\},$$

where $\bar{U}^{N,M}$ denotes the bilinear interpolant of the solution. These values are used to compute the approximate orders of global convergence using

$$Q_\varepsilon^{N,M} := \log_2(F_\varepsilon^{N,M}/F_\varepsilon^{2N,2M}).$$

The uniform global orders of convergence are estimated by computing

$$F^{N,M} := \max_{\varepsilon\in S} F_\varepsilon^{N,M}, \quad Q^{N,M} := \log_2(F^{N,M}/F^{2N,2M}),$$

with $S = \{2^0, 2^{-1}, 2^{-2}, \ldots, 2^{-30}\}$. The numerical results presented in Tables 1 and 2 are in line with our theoretical findings. In Table 3 we fix the value of the singular perturbation parameter to $\varepsilon = 2^{-16}$ and we take different values of $\theta = 2^{-20}, 2^{-18}, \ldots, 2^{10}$. We observe that the method is convergent but the maximum two-mesh differences are greater as θ increases and the orders of convergence have deteriorated.

Table 1 Numerical method (5): Computed two-mesh differences $F_\varepsilon^{N,M}$ and uniform differences $F^{N,M}$ with their corresponding orders of convergence $Q_\varepsilon^{N,M}$, $Q^{N,M}$ for problem (8) with $\theta = 1$.

	N=M=32	N=M=64	N=M=128	N=M=256	N=M=512	N=M=1024
$\varepsilon = 2^0$	0.742E-01 0.492	0.528E-01 0.639	0.339E-01 0.785	0.197E-01 0.882	0.107E-01 0.939	0.557E-02
$\varepsilon = 2^{-2}$	0.558E-01 0.777	0.326E-01 0.867	0.179E-01 0.920	0.944E-02 0.957	0.486E-02 0.978	0.247E-02
$\varepsilon = 2^{-4}$	0.373E-01 0.727	0.225E-01 0.855	0.125E-01 0.925	0.656E-02 0.961	0.337E-02 0.980	0.171E-02
$\varepsilon = 2^{-6}$	0.556E-01 1.284	0.228E-01 0.949	0.118E-01 0.974	0.602E-02 0.987	0.304E-02 0.993	0.153E-02
$\varepsilon = 2^{-8}$	0.698E-01 1.140	0.317E-01 1.164	0.141E-01 1.117	0.652E-02 1.064	0.312E-02 1.035	0.152E-02
$\varepsilon = 2^{-10}$	0.110E+00 0.836	0.615E-01 1.360	0.239E-01 1.376	0.922E-02 1.277	0.381E-02 1.173	0.169E-02
$\varepsilon = 2^{-12}$	0.861E-01 -.264	0.103E+00 0.881	0.562E-01 1.522	0.196E-01 1.568	0.660E-02 1.456	0.241E-02
$\varepsilon = 2^{-14}$	0.827E-01 -.033	0.847E-01 0.332	0.672E-01 1.145	0.304E-01 1.387	0.116E-01 1.445	0.427E-02
⋮	⋮	⋮	⋮	⋮	⋮	⋮
$\varepsilon = 2^{-30}$	0.827E-01 0.020	0.816E-01 0.301	0.662E-01 1.134	0.302E-01 1.381	0.116E-01 1.442	0.426E-02
$F^{N,M}$ $Q^{N,M}$	0.110E+00 0.085	0.103E+00 0.612	0.677E-01 1.121	0.311E-01 1.420	0.116E-01 1.063	0.557E-02

Remark 2. Given the initial large time derivatives visible in Figure 3 and also present in the bounds (4b) on the time derivatives of the solution, it is natural to consider a piecewise uniform mesh in time where the transition parameter is taken to be

Table 2 Numerical method (5): Computed two-mesh differences $F_\varepsilon^{N,M}$ and uniform differences $F^{N,M}$ with their corresponding orders of convergence $Q_\varepsilon^{N,M}$, $Q^{N,M}$ for problem (8) with $\theta = 100$.

	N=M=32	N=M=64	N=M=128	N=M=256	N=M=512	N=M=1024
$\varepsilon = 2^0$	0.587E-01 0.156	0.526E-01 0.273	0.436E-01 -.080	0.461E-01 -.020	0.467E-01 0.226	0.399E-01
$\varepsilon = 2^{-2}$	0.557E-01 0.108	0.517E-01 0.271	0.428E-01 -.108	0.462E-01 -.005	0.463E-01 0.236	0.394E-01
$\varepsilon = 2^{-4}$	0.781E-01 0.451	0.572E-01 0.363	0.444E-01 -.080	0.470E-01 0.011	0.466E-01 0.244	0.393E-01
$\varepsilon = 2^{-6}$	0.122E+00 0.800	0.703E-01 0.484	0.503E-01 0.006	0.501E-01 0.067	0.478E-01 0.265	0.398E-01
$\varepsilon = 2^{-8}$	0.122E+00 0.799	0.703E-01 0.502	0.497E-01 -.033	0.508E-01 0.064	0.486E-01 0.270	0.403E-01
$\varepsilon = 2^{-10}$	0.122E+00 0.798	0.703E-01 0.502	0.497E-01 -.032	0.508E-01 0.064	0.486E-01 0.270	0.403E-01
$\varepsilon = 2^{-12}$	0.122E+00 0.797	0.703E-01 0.502	0.497E-01 -.031	0.508E-01 0.064	0.486E-01 0.269	0.403E-01
$\varepsilon = 2^{-14}$	0.122E+00 0.797	0.703E-01 0.502	0.497E-01 -.031	0.507E-01 0.064	0.485E-01 0.269	0.403E-01
⋮	⋮	⋮	⋮	⋮	⋮	⋮
$\varepsilon = 2^{-30}$	0.122E+00 0.797	0.703E-01 0.502	0.497E-01 -.030	0.507E-01 0.064	0.485E-01 0.269	0.403E-01
$F^{N,M}$ $Q^{N,M}$	0.127E+00 0.849	0.703E-01 0.484	0.503E-01 -.016	0.509E-01 0.065	0.486E-01 0.269	0.404E-01

Table 3 Numerical method (5): Computed two-mesh differences $F_\varepsilon^{N,M}$ and their corresponding orders of convergence $Q_\varepsilon^{N,M}$ for problem (8) with $\varepsilon = 2^{-16}$.

	N=M=32	N=M=64	N=M=128	N=M=256	N=M=512	N=M=1024
$\theta = 2^{-16}$	0.317E-01 1.290	0.130E-01 1.171	0.576E-02 1.096	0.269E-02 1.051	0.130E-02 1.027	0.638E-03
$\theta = 2^{-12}$	0.266E-01 0.988	0.134E-01 1.265	0.557E-02 1.237	0.236E-02 1.156	0.106E-02 1.037	0.517E-03
$\theta = 2^{-8}$	0.656E-01 1.547	0.225E-01 1.542	0.771E-02 1.402	0.292E-02 1.252	0.123E-02 1.146	0.553E-03
$\theta = 2^{-4}$	0.904E-01 -.209	0.105E+00 0.943	0.544E-01 1.681	0.170E-01 1.778	0.494E-02 1.701	0.152E-02
$\theta = 2^0$	0.827E-01 -.007	0.831E-01 0.317	0.667E-01 1.140	0.303E-01 1.384	0.116E-01 1.443	0.427E-02
$\theta = 2^2$	0.113E+00 0.449	0.829E-01 0.280	0.683E-01 0.946	0.355E-01 1.158	0.159E-01 1.214	0.685E-02
$\theta = 2^4$	0.127E+00 0.714	0.772E-01 0.162	0.690E-01 0.553	0.470E-01 0.744	0.281E-01 0.869	0.154E-01
$\theta = 2^6$	0.132E+00 0.932	0.694E-01 0.306	0.562E-01 0.069	0.536E-01 0.231	0.456E-01 0.430	0.339E-01
$\theta = 2^8$	0.890E-01 0.476	0.640E-01 0.167	0.570E-01 0.251	0.479E-01 0.093	0.449E-01 -.075	0.473E-01
$\theta = 2^{10}$	0.437E-01 0.090	0.411E-01 -.263	0.493E-01 -.108	0.532E-01 0.023	0.523E-01 0.189	0.459E-01

$$\tau_t := \min\{T/2, (1/\theta)\ln M\}, \tag{9}$$

and to distribute uniformly $M/2+1$ points in the time subdomains $[0,\tau_t]$ and $[\tau_t, T]$. We repeat only two of the previous Tables 2 (where $\theta = 100$) and 3 (where $\varepsilon = 2^{-16}$); their companion Tables are 4 and 5. We observe an improvement in the numerical results compared to using a uniform mesh in time. The question of whether the inclusion of a piecewise-uniform mesh in time produces a parameter-uniform (with respect to both ε and θ) remains an open question.

Table 4 Finite difference scheme (5) coupled with a piecewise-uniform mesh in time (9): Computed two-mesh differences $F_\varepsilon^{N,M}$ and uniform differences $F^{N,M}$ with their corresponding orders of convergence $Q_\varepsilon^{N,M}$, $Q^{N,M}$ for problem (8) with $\theta = 100$.

	N=M=32	N=M=64	N=M=128	N=M=256	N=M=512	N=M=1024
$\varepsilon = 2^{0}$	0.844E-01 0.579	0.565E-01 0.738	0.339E-01 0.886	0.183E-01 1.006	0.912E-02 0.830	0.513E-02
$\varepsilon = 2^{-2}$	0.917E-01 0.630	0.593E-01 0.772	0.347E-01 0.904	0.185E-01 1.014	0.919E-02 0.860	0.506E-02
$\varepsilon = 2^{-4}$	0.881E-01 0.243	0.745E-01 1.012	0.369E-01 0.996	0.185E-01 0.925	0.975E-02 0.881	0.529E-02
$\varepsilon = 2^{-6}$	0.127E+00 0.594	0.840E-01 0.266	0.699E-01 1.139	0.317E-01 1.220	0.136E-01 1.104	0.634E-02
$\varepsilon = 2^{-8}$	0.127E+00 0.632	0.819E-01 0.298	0.666E-01 0.941	0.347E-01 1.093	0.163E-01 1.101	0.758E-02
$\varepsilon = 2^{-10}$	0.127E+00 0.651	0.808E-01 0.287	0.662E-01 0.938	0.346E-01 1.092	0.162E-01 1.100	0.757E-02
$\varepsilon = 2^{-12}$	0.127E+00 0.661	0.802E-01 0.281	0.660E-01 0.936	0.345E-01 1.091	0.162E-01 1.100	0.756E-02
$\varepsilon = 2^{-14}$	0.127E+00 0.665	0.800E-01 0.278	0.659E-01 0.935	0.345E-01 1.090	0.162E-01 1.099	0.756E-02
$\vdots$	$\vdots$	$\vdots$	$\vdots$	$\vdots$	$\vdots$	$\vdots$
$\varepsilon = 2^{-30}$	0.127E+00 0.670	0.797E-01 0.275	0.658E-01 0.934	0.345E-01 1.090	0.162E-01 1.099	0.756E-02
$F^{N,M}$ $Q^{N,M}$	0.141E+00 0.565	0.953E-01 0.448	0.699E-01 1.007	0.348E-01 1.095	0.163E-01 1.096	0.761E-02

Table 5 Finite difference scheme (5) coupled with a piecewise-uniform mesh in time (9): Computed two-mesh differences $F_\varepsilon^{N,M}$ and their corresponding orders of convergence $Q_\varepsilon^{N,M}$ for problem (8) with $\varepsilon = 2^{-16}$.

	N=M=32	N=M=64	N=M=128	N=M=256	N=M=512	N=M=1024
$\theta = 2^{2}$	0.113E+00 0.449	0.829E-01 0.280	0.683E-01 0.946	0.355E-01 1.158	0.159E-01 1.214	0.685E-02
$\theta = 2^{4}$	0.124E+00 0.628	0.805E-01 0.227	0.687E-01 0.671	0.432E-01 0.789	0.250E-01 0.837	0.140E-01
$\theta = 2^{6}$	0.127E+00 0.679	0.794E-01 0.228	0.678E-01 0.675	0.425E-01 0.793	0.245E-01 0.840	0.137E-01
$\theta = 2^{8}$	0.128E+00 0.693	0.791E-01 0.227	0.676E-01 0.675	0.423E-01 0.794	0.244E-01 0.840	0.136E-01
$\theta = 2^{10}$	0.128E+00 0.697	0.790E-01 0.227	0.675E-01 0.675	0.423E-01 0.794	0.244E-01 0.841	0.136E-01

References

1. C. de Falco and E. O'Riordan, Interior layers in a reaction–diffusion equation with a discontinuous diffusion coefficient, *Int. J. Numer. Anal. Mod.*, 7(3), 2010, 444–461.
2. P.A. Farrell, A.F. Hegarty, J.J.H. Miller, E. O'Riordan and G.I. Shishkin, *Robust computational techniques for boundary layers*, Chapman and Hall/CRC Press, (2000).
3. J.L. Gracia and E. O'Riordan, A singularly perturbed parabolic problem with a layer in the initial condition, *Appl. Math. Comput.*, 219 (2), 2012, 498–510.
4. J.L. Gracia and E. O'Riordan, A singularly perturbed convection-diffusion problem with a moving pulse, *J. Comp. Appl. Math.*, 321, 2017, 371–388.
5. O.A. Ladyzhenskaya, V.A. Solonnikov and N.N. Ural'tseva, *Linear and quasilinear equations of parabolic type*, Transactions of Mathematical Monographs, 23, American Mathematical Society, (1968).
6. J.J.H. Miller, E. O'Riordan and G.I. Shishkin and L.P. Shishkina, Fitted mesh methods for problems with parabolic boundary layers, *Mathematical Proceedings of the Royal Irish Academy*, 98A, 1998, 173–190.